Capicua maintains anterior-posterior axis in *Blattella germanica* ovaries.

Nashwa Elshaer[1§], Jorge Escudero[1], Maria-Dolors Piulachs[1]*****

[1] *Institute of Evolutionary Biology (CSIC-University Pompeu Fabra). Passeig Marítim de la Barceloneta, 37. 08003 Barcelona, Spain*

[§] Present address: *Department of Plant Protection, Faculty of Agriculture, Zagazig University, 44511 Zagazig, Egypt*

***** Corresponding author: Maria-Dolors Piulachs (mdolors.piulachs@ibe.upf-csic.es)

Abstract

The establishment of the symmetry axis is crucial for the development of all organisms. In insects, this process begins early in oogenesis with the correct distribution of the mRNAs and proteins in the oocyte. One of the proteins that contribute to organizing this distribution is Capicua (Cic). Cic has been studied in *Drosophila melanogaster* oogenesis and embryo development, it is maternally expressed and is required to establish the dorso-ventral axis, acting as a repressor transcription factor. Although the sequence of Cic is conserved across species, its function in other types of insect ovaries is still unknown. We wondered whether the function of Cic in insects has been maintained through evolution despite the ovary type or if it has been modified in parallel to the ovary evolution. To address this, we studied the Cic function in a phylogenetically basal insect, the cockroach *Blattella germanica*, a species with panoistic ovaries. The Cic sequence of *B. germanica* shares 80% identity with *D. melanogaster* Cic. Our findings indicate that Cic is essential for oocyte development as it is involved in establishing the anterior-posterior axis.

Keywords

oocyte polarity, *Drosophila*, oogenesis, panoistic ovary

1. Introduction

Oogenesis is a crucial process in animal kingdom, as it ensures the continuity of the species. Therefore, it must be regulated with great precision. A good model for studying oogenesis is the insect ovary and, especially, the panoistic ovary which is characterized by the absence of nurse cells escorting the germinal cell or oocyte. Instead of this organization, each ovarian follicle only consists in an oocyte surrounded by a monolayered follicular epithelium (Büning, 1994). The panoistic ovary is characteristic of phylogenetically basal insects like the cockroach *Blattella germanica*, our insect model (Belles et al., 2024), and it is the most common ovarian type in invertebrates and vertebrates (Telfer, 1975). In addition, during *B. germanica* oogenesis, the basal ovarian follicle is the only one that matures in each reproductive cycle, while the other ovarian follicles remain in the vitellarium, waiting to occupy the basal position in subsequent cycles (Belles et al., 2024; Donato Tanaka & Piulachs, 2012; Irles & Piulachs, 2014). Ovarian follicles in meroistic ovaries, like those of *Drosophila melanogaster* ovary, are clearly asymmetric, as they are formed by a cluster of nurse cells and the oocyte, both surrounded by a monolayer of follicular cells (Büning, 1994). The dorso-ventral asymmetry is established in the oocyte at mid oogenesis, when the nucleus takes a dorsal-anterior position (Roth & Lynch, 2012). In contrast, in panoistic ovaries, like those of *B. germanica*, ovarian follicles are more symmetric due to the absence of nurse cells and to the short migration of oocyte nucleus which moves late in the oogenesis from the center to a mid-ventral position of the oocyte (Tanaka, 1973). This discrete change in the nucleus position and the oval shape of young panoistic ovarian follicles makes difficult to distinguish the DV axis in them. In *B. germanica*, however, the asymmetric distribution of F-actins in the oocyte membrane, and the maintenance of patency in the ventral follicular cells, facilitates the identification of the ventral side of the basal ovarian follicle (Zhang & Kunkel, 1992).

These asymmetries in the oocyte morphology have a correspondence in the asymmetric distribution of the mRNAs encoding for patterning factors (Medioni et al., 2012). The distribution of these patterning factors has been thoroughly studied in holometabolan insects (Fonseca et al., 2009; Wilson et al., 2011; Wilson & Dearden, 2013), especially in

D. melanogaster (Roth & Lynch, 2012; Shin & Hong, 2014), in relation to embryogenesis, where minor modifications in mRNA or protein localization in the oocyte may be lethal for the embryo. We have adopted the panoistic ovary of *B. germanica* as model with the aim of unveiling key factors involved in establishing and maintaining the distribution of the mRNAs in the oocyte, and we have started by studying the function of the transcription factor Capicua (derived from the Catalan term meaning "head-and-tail", Cic) in this basal ovary type. *cic-mRNA* encodes for an HMG-box protein that acts as a transcriptional factor repressor, and is structurally conserved from cnidarians to vertebrates (Jiménez et al., 2000; Lam et al., 2006; Rodrıguez-Muñoz et al., 2022). In *D. melanogaster*, *cic* has been reported as a maternally expressed gene that is required for the establishment of DV patterning of the eggshell and the embryonic termini during embryogenesis (Goff et al., 2001; Jiménez et al., 2000; Rodrıguez-Muñoz et al., 2022). In humans and mice, Cic is involved in the development of the nervous system, lung development, abdominal wall closure, or in bile acid homeostasis (Jiménez et al., 2012; C. J. Lee et al., 2002; Y. Lee, 2020; Y. Lee et al., 2011). In addition, Cic inactivation has been related with different cancer processes in humans (Alentorn et al., 2012; Herraiz et al., 2014; Kim et al., 2018; Y. Lee, 2020).

In this study, our results will show that Cic in the panoistic ovary of *B. germanica*, is necessary to maintain the anterior posterior axis in the ovarian follicles as is regulating the stabilization of the F-actin in the oocyte, a function that is exerted early during the oocyte development.

2. Materials and Methods

2.1. Insects

Blattella germanica (L.) specimens were obtained from a colony reared in the dark at 29 ± 1°C and 60–70% relative humidity (Bellés et al., 1987). Adult females were maintained with males during all the first gonadotrophic cycle, and mating was confirmed at the end of the experiments by assessing the presence of spermatozoa in the spermathecae. All

dissections and tissue sampling were carried out on carbon dioxide-anesthetized specimens. Tissues were frozen on liquid nitrogen and stored at -80ºC until use.

2.2. Cloning and Sequencing

A fragment of *B. germanica capicua* (*cic*) sequence (493 bp) was obtained from an mRNA library available in the laboratory. The sequence of *cic* was completed by 3´- and 5´- rapid amplification of cDNA ends (RACE), according to the manufacturer protocol (Ambion, Huntingdon, Cambridgeshire, UK). The amplified fragments were cloned into the pSTBlue-1 vector (Novagen, Madison, WI, USA) and sequenced by Sanger (accession number in NCBI: LN623700).

2.3. Sequence comparisons and phylogenetic analysis

Sequences of Cic protein from insects were obtained from GenBank. The search was enlarged by Blast using the *B. germanica* and *D. melanogaster* Cic as queries. The sequences used in the phylogenetical analysis are listed in Supplementary table 1. Protein sequences were aligned using ClustalX (Larkin et al., 2007). The resulting alignment was analyzed by the PHYML 3.0 program (Guindon & Gascuel, 2003) based on the maximum-likelihood principle, using a JTT matrix, four substitution rate categories with a gamma shape parameter of 1.444, and using empirical base frequencies and estimating proportions. The data was bootstrapped for 100 replicates using PHYML 3.0.

2.4. RNA extraction and expression studies

Total RNA was isolated using GenElute Mammalian Total RNA kit (Sigma, Madrid, Spain). An amount of 400 ng from each RNA extraction was DNAse treated (Promega, Madison, WI, USA) and reverse transcribed with Superscript II reverse transcriptase (Invitrogen, Carlsbad CA, USA) and random hexamers (Promega). RNA quantity and quality was estimated by spectrophotometric absorption at 260/280 nm in a Nanodrop Spectrophotometer ND-1000® (NanoDrop Technologies, Wilmington, DE, USA).

Expression of *cic* was determined by quantitative real-time PCR (qRT-PCR) in the last nymphal instar and in the adult stage during the first gonadotrophic cycle. PCR primers used in qRT-PCR expression studies were designed using the Primer Express 2.0

software (Applied Biosystems, Foster City, CA, USA), and are detailed in Supplementary table 2. The *B. germanica actin-5c* mRNA (Accession number AJ862721), was used as a reference. qRT-PCR reactions were performed using the SYBR Green Supermix (BioRad) containing 200 nM of each specific primer. Amplification reactions were carried out at 95ºC for 2 min, and 40 cycles of 95ºC for 15 s and 60ºC for 30s, using MyIQ Single Color RTPCR Detection System (BioRad). After the amplification phase, a dissociation curve was carried out to ensure that there was only one product. Levels of mRNA were calculated relative to the respective reference gene, using the $2^{-\Delta\Delta Ct}$ method and $2^{-\Delta Ct}$ method (Irles et al., 2009; Livak & Schmittgen, 2001; Maestro et al., 2005). Results are given as copies of mRNA per 1000 copies of *actin-5c* mRNA and correspond to three biological replicates.

2.5. RNA interference

To knockdown *cic*-mRNA and asses the specificity of the phenotype, two different dsRNAs (ds*cic*-1 and ds*cic*-2) were designed and synthesized as previously described (Ciudad et al., 2006). The ds*cic*-1 was 324 bp in length (from nucleotides 5,874 to 6,197) and the second one, ds*cic*-2 392 bp (from nucleotides 4,366 to 4,757). As dsRNA control (dsMock) a fragment (300 bp) of the sequence of *Autographa californica nucleopolyhedrovirus* (GenBank: K01149) was used. The corresponding cDNAs were amplified by PCR and cloned into pSTBlue-1 vector. Newly emerged sixth nymphal instar females or newly emerged adult females were independently treated with 1 µg of ds*cic*-1 or 1 µg ds*cic*-2. As the same ovary phenotype was found using both dsRNA, we will refer to RNAi treatments as ds*cic*. The same dose and conditions used in ds*cic* treatments were applied to dsMock-treated females.

2.6. Immunohistochemistry

After dissection, ovaries were fixed immediately for 2 h with 4% paraformaldehyde in PBS, washed in PBT (PBS; 0.3% Triton-X100), treated with 50 µg/ml proteinase K for 2 min, washed for 2 min in 2 mg/mL glycine in PBT, washed for 10 min in PBT and fixed again for 20 min in the same solution. Then the ovaries were washed three times for 10 min with PBT (PBS; 0.1% Triton-X100, 0.1% BSA). After three washes with PBT the

ovaries were saturated for 1 h at room temperature in PBTBN (PBS; 0.1% Triton-X100, 0.5% BSA and 5% normal goat serum), and incubated overnight at 4º C with the primary antibody. The primary antibodies used were rat anti-Cic (1:200, generated against the C-terminal half of *D. melanogaster* Cic protein, kindly provided by Jordi Casanova; Molecular Biology Institute of Barcelona, CSIC), mouse anti-EGFR (15µg/mL) and mouse anti-Eya (1:50). Tissues were washed with PBTBN three times and incubated for 2 h with Alexa-Fluor 647 goat anti- mouse or anti-rat IgG (Molecular Probes, Carlsbad, CA, USA) diluted 1:400 in PBTBN. For F-actin visualization, ovaries were incubated for 20 min in 1µg/mL phalloidin-TRITC (Sigma), and after washing they were mounted in UltraCruz™ Mounting Medium (Santa Cruz Biotechnology®, inc., Delaware CA, USA), which contains DAPI for DNA staining. Samples were observed by epifluorescence microscopy using a Zeiss AxioImager.Z1 microscope (ApoTome), using the software Zen 2012, blue edition (Carl Zeiss MicroImaging).

2.7. Statistics

Data are expressed as mean ± standard error of the mean (S.E.M.). Statistical analysis of gene expression values was carried out using the REST 2008 program (Relative Expression Software Tool V 2.0.7; Corbett Research) (Pfaffl et al., 2002). This program makes no assumptions about the distributions, evaluating the significance of the derived results by Pair-Wise Fixed Reallocation Randomization Test tool in REST (Pfaffl et al., 2002). The sample group was considered significantly different from the control group when P(H1) = 0.000.

Results

3.1. *Blattella germanica* has a structurally conserved Capicua ortholog

capicua from *B. germanica* (*cic*), was amplified, cloned and sequenced from ovarian tissues. The complete sequence of *cic* has 7,631 bp with an ORF encoding for a protein of 2,279 amino acids (nucleotide positions 553-7,392). *B. germanica* Cic possesses an HMG-box domain (from amino acid 1,206 to 1,274) characteristic of Cic proteins that is

highly conserved when compared to Cic from other insect species, like *Acromyrmex echinator*. (98%), or *D. melanogaster* (80%).

A maximum-likelihood analysis of Cic sequences from insects available in the literature and databases, gave a phylogenetic tree (Figure 1) with two clades, clearly separated corresponding to hemimetabolous and holometabolous insect species. The topology of the phylogenetic tree of Cic sequences overlaps with the currently accepted phylogeny of the included species (Misof et al., 2014) . All insect orders appeared grouped with high consistence in the nodes. It is worth noting that the Cic sequences of from Lepidoptera and Diptera form two clusters with the longer branches, indicating more extensive changes and consequently a faster rate of divergence compared to the rest of other insect orders.

3.3. *cic* is highly expressed in the ovary during the last nymphal instar

The expression of *cic* mRNA was studied in different tissues from 3-day-old adult females, namely the ovary, thoracic ganglia, colleterial glands, fat body, brain, and midgut (Figure 2A). *cic* is expressed in all tissues analyzed, showing the highest levels in the brain and ovary. In ovaries, the expression pattern of *cic* does not show significant changes (Figure 2B). In general, in ovaries from sixth instar nymphs, the levels of *cic* mRNA are higher than in adults and the last days of the fifth nymphal instar. After the imaginal molt, the expression of *cic* tends to decrease, reaching the lowest levels just before oviposition (Figure 2B). These expression patterns suggest that the main function of Cic in the ovary occurs during the last nymphal instar.

3.4. Cic protein localizes in somatic and germ cells

A heterologous antibody against Cic protein of *D. melanogaster* was used to localize Cic in *B. germanica* ovaries. Cic labeling was detected in all ovarian follicles through the ovariole, and in both germinal and somatic cells (Figure 2C). However, there is a clear differential distribution of Cic in the growing oocyte. In the basal follicle of 0-day-old sixth instar nymphs, Cic labeling appears as a thin layer close to the oocyte membrane (Figure 2D), being less intense in the anterior and posterior oocyte poles. Later, in 6-day and 8-day-old sixth instar nymphs (Figure 2E and F respectively), Cic labeling spreads

through the ooplasm and becomes more intense, even accumulating as a thick layer in the boundary of the oocyte. This labeling is displayed in all ovarian follicles, from the basal to the most distal, as well as in the germarium (Figure 2C). In 8-day-old sixth instar nymphs, as the female approaches the adult moult, Cic labeling appears in the oocyte nucleus, spreads with a faint signal throughout the oocyte cytoplasm, although the signal increase in the oocyte membrane (Figure 2F'). After the imaginal moult, Cic labeling in the oocyte becomes very faint (Figure 2G). Concerning follicular cells, in 8-day-old sixth instar nymphs, Cic appears abundant in the cytoplasm (Figure 2H), whereas in 0-day-old adults, labeling in the follicular cells became fainter and concentrated in the basal pole (Figure 2I). Overall, the findings show that the Cic localization in the ovary undergoes sequential and relevant changes, indicating that it has distinct functions during oocyte maturation.

3.5. Cic is involved in oogenesis of *B. germanica*.

To unveil the functions of Cic in the panoistic ovaries of *B. germanica*, 1µg of ds*cic* was injected to two different experimental models: females treated at 0-day-old adult or at 0-day-old sixth instar nymphs. In both experiments, the females were maintained with untreated males until oviposition.

In females treated just after the emergence to the adult stage, the ovarian mRNA levels for *cic* were measured 48h after the treatment, exhibiting a 27% of reduction. This depletion that was sufficient to perturb oviposition and embryogenesis in early stages. Of the 45 treated females, 18% did not oviposit, and 4% were died before oviposition. 78% (n= 35) of treated females oviposited formed ootheca properly. However, most of them (60%) abandoned the ootheca 48–72 h after it formed, whilst the remaining females maintained the ootheca attached to the genital pouch, which gave rise to nymphs that emerged normally without delays. The females treated as 0-day-old sixth instar nymphs (n = 65), molted normally to the adult 8 days later, similar to the dsMock-treated nymphs. At the end of the gonadotrophic cycle, all dsMock-treated females oviposited and had a normal ootheca, whereas none of the ds*cic*-treated females did. Expression levels of *cic* mRNA in the ovary were measured every 48 h during the nymphal instar and just after adult emergence (Figure 3A). Results showed that only in 8-day-old ds*cic*-treated sixth

instar nymphs, the expression of *cic* mRNA tended to decrease when compared to dsMock-treated nymphs (Figure 3A). Moreover, in the basal ovarian follicle of these 8-day-old ds*cic*-treated sixth instar nymphs (Figure 3B) no Cic protein labeling was detected in the ovarian follicle, and only a faint signal was noticed in the basal pole of follicular cells (Figure 3B, B'), when compared with the basal ovarian follicle from 8-day-old dsMock-treated sixth instar nymphs (Figure 3C, C'). The most important effect observed in these ds*cic*-treated females was the transformation of the basal ovarian follicle, which appeared elongated with defects affecting mainly the anterior and posterior poles (Figure 3B), a morphology that is very different from that of basal ovarian follicles of dsMock-treated females, which have the typical elliptical shape (Figure 3C). To analyze this phenotype due to the *cic* mRNA depletion, a new batch of ds*cic*-treated (n = 20) and dsMock-treated (n = 20) 0-day-old sixth instar nymphs was prepared to examine the ovarian follicle at different ages, in the last nymphal instar and in the adult.

The basal ovarian follicles from 8-day-old ds*cic*-treated sixth instar nymphs appeared elongated (Figure 3B and 4), and the anterior pole of the oocyte became narrow and penetrates into the lumen of the stalk (Figure 4A, B). Conversely, the posterior pole showed a "fishtail-like" morphology (Figure 4C, D). Later, in 3-day-old adults, the basal ovarian follicle of ds*cic*-treated females appeared still more elongated (Figure 4E) and the apical pole of the oocyte that penetrates in the lumen of the stalk appeared engulfed by those follicular cells that localize close to the anterior pole of the ovarian follicle (Figure 4 F, G).

In general, in both poles of the younger oocytes in the vitellarium of dsMock-treated females, show high amounts of F-actins constituting the microtubule organization center (MTOC), with a network of F-actins connecting with this structure (Figure 4H), which usually disappears in the basal oocytes. However, the MTOC remains present and strongly labeled in the basal oocyte of 8-day old ds*cic* treated sixth instar nymphs (Figure 4D, I, J). It is also preserved and significantly larger in the basal ovarian follicle of 3-day-old adults from the ds*cic*-treated group (Figure 4K).

In ovaries of 7-day-old adults, when the chorion synthesis begins in dsMock-treated females, all the ovarioles of the ds*cic*-treated specimens lost the basal and the sub-basal oocytes, remaining only the sheath of follicular epithelium that covered the oocytes

(Figure 4L, arrows). Moreover, the more distal oocytes that still remain in the vitellarium exhibit an unusual hourglass morphology; possibly due to a generalized enrichment of F-actins in the ooplasm (Figure 4M).

3.7. Depletion of *cic* mRNA affects the immature ovarian follicles

Observing in detail all ovarian follicles in the ovariole, of these 8-day-old ds*cic*-treated sixth instar nymphs (Figure 5), we observed that the nucleus in the oocytes is not centered, as occurs in controls (Figure 5A). Rather it takes a posterior position, in the basal oocyte (Figure 5B) and in the immature oocytes within the ovariole as well (Figure 5C, D and E). It seems that the nucleus was pushing the oocyte towards the posterior pole of the ovarian follicle, and as a consequence many oocytes can be encapsulated in one ovarian follicle (Figure 5E). This is facilitated by the absence of follicular cells in the poles and by the absence of stalk cells separating young ovarian follicles, which determined the fusion of the oocyte membranes, thus giving the aspect of a single oocyte with more than one nucleus (Figure 5C, D and E, arrowhead). Moreover, the absence of the stalk connecting successive ovarian follicles leads to a general disorganization of the ovariole that especially affects those ovarian follicles that just have been formed and are ready to leave the germarium.

As a consequence of these dysfunctions, in older adult females (7-day-old), it can be observed that the malformed basal follicle has fallen and is lost into the oviduct, without reaching complete maturation (figure 4L).

3.8. Depletion of *cic* mRNA affects other pathways involved in insect oogenesis

The complex phenotype produced by the depletion of *cic* mRNA suggests that this protein could interact with other pathways related with cell proliferation and stalk formation. Even with the EGFR signaling, as the anterior-posterior polarity in the ovarian follicles is disrupted in *EGFR*-depleted nymphs, which provokes the disorganization of the ovariole (Elshaer & Piulachs, 2015).

The expression of *EGFR* in ovaries from 8-day-old sixth instar nymphs that had been treated with ds*cic*, tended to decrease, although the differences with respect to controls were not statistically significant (Figure 6A). However, the localization of EGFR protein

in these treated nymphs appeared modified compared to dsMock-treated nymphs (Figure 6). In ds*cic*-treated females, EGFR labeling is restricted to the mid region of the basal oocyte and around the nucleus (Figure 6C), while in dsMock-treated nymphs it spreads over the cytoplasm and concentrates around and within the nucleus (Figure 6B), concentrated in the nucleus membrane.

In relation to proliferation, we measured the expression of *Hpo*, which resulted significantly down-regulated (0.351-fold change) in *cic* knockdowns nymphs (Figure 6A), although we did not detect higher levels of proliferation in the follicular epithelia of these specimens. In relation to the Hippo pathway, and related to the loss of stalk formation, we analyzed the expression of *Notch* (*N*) and *Delta* (*Dl*), from Notch pathway (Irles et al., 2016; Irles & Piulachs, 2014). As expected, the expression of *N* tends to decrease, while its ligand *Dl* is significantly up-regulated (1.161-fold change) in ds*cic*-treated last instar nymphs (Figure 6A).

Finally, the modifications observed in the anterior-posterior poles in ovarian follicles from ds*cic*-treated sixth instar nymphs, suggested to look for genes that contribute to drive the terminal position in *D. melanogaster* egg chambers and in embryos. Therefore, we examined the response of *tailless* (*tll*) (Figure 6A). Results show that in ds*cic* knockdowns, the expression of *tll* mRNA levels are significantly down-regulated (0.355 of fold change). We additionally measured the expression of the transcription factor *Dorsal* (DL), which is required for the determination of dorsal-ventral polarity, observing that it decreased significantly (0.408-fold change) (Figure 6A).

4. Discussion

Cic sequence is highly conserved among animals, from cnidarians to vertebrates (Lam et al., 2006; C. J. Lee et al., 2002) and in most insects, including *B. germanica*, it is expressed as a single isoform, while in *D. melanogaster* and in mammals at least two isoforms are expressed with alternative domains (Jiménez et al., 2012; Rodrıguez-Muñoz et al., 2022). We have demonstrated that *B. germanica cic* is particularly well expressed in the brain and in the ovaries. The high levels of *cic* expression in *B. germanica* brain suggest that Cic might have an important role in the development of the central nervous

system (CNS), a function described for Cic in vertebrates, which show a high expression in immature granule cells in the cerebellum, in the hippocampus and in the olfactory bulb (C. J. Lee et al., 2002). while mutations in the *cic* gene determining an absence of the protein, are detected in oligodendroglial tumors (Alentorn et al., 2012; Chan et al., 2014; Kim et al., 2015; Y. Lee, 2020). In the present study, however, we have focused on the expression and function of Cic in the ovaries. Indeed, the role of Cic in insects has been thoroughly documented in *D. melanogaster* in relation to oogenesis and to the specification of terminal regions in the embryo, as the loss of Cic function results in a dorsalization of the eggshell and the embryo (Atkey et al., 2006; Goff et al., 2001; Jiménez et al., 2000; Rodrıguez-Muñoz et al., 2022) and affects the anterior-posterior embryonic axis (Andreu et al., 2012). In *Tribolium castaneum*, Cic is necessary for anterior-posterior patterning without any obvious impact on dorsoventral pattern formation and its depletion causes terminal anlagen to enlarge (Prido□ Hl et al., 2017).

In the panoistic ovary of *B. germanica*, Cic protein accumulates in the basal oocytes of sixth instar nymphs as they progress in the instar. However, after the imaginal moult, labeling for this protein in the basal oocytes become very weakly. This confirms that in the panoistic ovary, the most important steps for oogenesis and further oocyte maturation occur during the last nymphal instar, thus when the female reach the adult stage, the basal follicles are ready to incorporate storage proteins into the oocyte and to complete growth (Belles et al., 2024; Ciudad et al., 2006; Donato Tanaka and Piulachs, 2012; Herraiz et al., 2014; Irles and Piulachs, 2014). According to our findings, Cic plays a crucial role in oogenesis, which occurs prior to the ovarian follicle reaching maturity, and its depletion causes female sterility. Equivalent observations have been reported for *D. melanogaster* (Jiménez et al., 2000), where Cic has a fundamental function in oocyte development and its depletion determines female sterility as well. However, the mechanisms underlying this macroscopic phenotype differ between the two species and in both ovaries types.

Females of *D. melanogaster* mutants for Cic, are able to oviposit, but the eggs have defects in the eggshell and the embryos start developing but they are not able to complete it and to hatch (Goff et al., 2001; Rodríguez-Muñoz et al., 2022). Conversely, in *B. germanica*, *cic*-depleted females do not oviposit correctly, as the oocyte cannot complete their development.

Cic is required to maintain the anterior-posterior axis within the panoistic ovary of *B.germanica*. As a depletion of *cic* mRNA triggers morphological modifications in the anterior-posterior poles of the basal ovarian follicles as a result of important changes in the distribution of F-actin microfilaments, in both the oocyte and in the follicular cells. Actins are the main component of the cytoskeleton and are crucial in different cellular processes, like cell division and shaping (Riparbelli & Callaini, 1995; Sun & Schatten, 2006). Related with the change in the F-actins distribution in the ds*cic*-treated females, MTOCs are maintained in the poles of the basal oocyte in the transition from nymph to adult, and a network of F-Actins can be detected connecting the both MTOCs in poles. Usually, the MTOCs disappeared from the basal oocytes in the last days of the sixth nymphal instar, and they are never detected in the basal oocytes from a *B. germanica* adult female. The importance of the MTOC, which is an important organizer of the microtubule network, in the distribution of mRNAs and proteins into the oocyte has been thoroughly demonstrated in *D. melanogaster* (Cooley & Theurkauf, 1994; Roth & Lynch, 2012). The actin cytoskeleton also provides the oocyte growth and differentiation (Riparbelli & Callaini, 1995) and polarity establishment (Sun & Schatten, 2006). Conversely, the information regarding the role of the MTOC in the distribution of proteins or mRNAs in a panoistic ovary is scarce.

We posit that the maintenance of this network of F-actin in ds*cic*-treated females affects the distribution of EGFR protein that appears modified in basal oocytes, as the protein appears restricted to the middle region of the oocyte, and is not spread by all the cytoplasm as happens in control basal oocytes. The restriction and lack of EGFR protein may explain the fusion of immature oocytes membranes in ds*cic* specimens of *B. germanica*. Likewise, depletion of EGFR cause increasing the rate of germ cells mitosis at the expense of decreasing somatic follicular cells causing oocytes overlapping and fusions (Elshaer & Piulachs, 2015).

The results obtained by the depletion of *cic* affecting the stalk formation, the polarity of the oocyte or cell proliferation, suggested that Cic might be interacting with different pathways contributing to oocyte development. For example, it has been reported that Notch pathway is involved in the formation of the stalk (Irles & Piulachs, 2014). In *D. melanogaster*, the inhibition of Cic by EGFR results in de-repressing Hippo which acts

on cell proliferation (Herranz et al., 2012). In contrast, in *B. germanica*, depletion of *cic* results in Hpo down-regulation, although the follicular epithelium continues proliferating. This suggests that Notch levels in the ovarian follicle maintain an adequate level of proliferation, as reported previously (Irles & Piulachs, 2014), where the follicular epithelium continues to proliferate in the absence of Hpo due to the Notch being maintained in the follicular cells.

Moreover, the depletion of *Cic* seems to modify the expression of those genes that in *D. melanogaster* are required to establish the anterior-posterior polarity or the DV axis (like *oskar, tailless, staufen, bruno and dorsal*) (Lynch & Roth, 2011; Roth & Lynch, 2009), as they were down-regulated in *B.germanica*. It will be necessary to investigate the function of all these genes in a panoistic ovary, where the polarity of the oocyte differs greatly of that of a meroistic oocyte, and unveil how its function has modified through the evolution. The main function described for Cic was to be a transcriptional repressor, in *D. melanogaster* and other species (Jiménez et al., 2000). However, our results suggests that Cic in the panoistic ovary, the ancestral ovary type, might act as inducer of the transcriptional activity. To unveil how was produced the transition from a transcriptional inductor to a transcriptional repressor, will be necessary to study the Cic function in different insect models and in relation with the other pathways that controls oocyte organization and maturation.

Acknowledgments

The work was funded with the grant PID2021-122316OB-I00 from the MICIU/AEI /10.13039/501100011033 and ERDF, a way of making Europe. We are grateful to Xavier Belles for the critical reading of the manuscript. The authors acknowledge the support of the publication fee by CSIC Open Access Publication Support Initiative through its Unit of Information Resources for Research (URICI).

References

Alentorn, A., Sanson, M., & Idbaih, A. (2012). Oligodendrogliomas: new insights from the genetics and perspectives. *Current Opinion in Oncology*, *24*(6), 687–693. https://doi.org/10.1097/CCO.0B013E328357F4EA

Andreu, M. J., González-Pérez, E., Ajuria, L., Samper, N., González-Crespo, S., Campuzano, S., & Jiménez, G. (2012). Mirror represses pipe expression in follicle cells to initiate dorsoventral axis formation in *Drosophila*. *Development (Cambridge, England)*, *139*(6), 1110–1114. https://doi.org/10.1242/DEV.076562

Atkey, M. R., Lachance, J. F. B., Walczak, M., Rebello, T., & Nilson, L. A. (2006). Capicua regulates follicle cell fate in the *Drosophila* ovary through repression of mirror. *Development (Cambridge, England)*, *133*(11), 2115–2123. https://doi.org/10.1242/DEV.02369

Bellés, X., Casas, J., Messeguer, A., & Piulachs, M. D. (1987). In vitro biosynthesis of JH III by the corpora allata of adult females of *Blattella germanica* (*L*). *Insect Biochemistry*, *17*(7), 1007–1010. https://doi.org/10.1016/0020-1790(87)90111-9

Belles, X., Maestro, J. L., & Piulachs, M. D. (2024). The German cockroach as a model in insect development and reproduction in an endocrine context. *Advances in Insect Physiology*, *66*(1), 1–47. https://doi.org/https://doi.org/10.1016/bs.aiip.2024.03.001

Büning, J. (1994). The Insect Ovary. *The Insect Ovary*. https://doi.org/10.1007/978-94-011-0741-9

Chan, A. K. Y., Pang, J. C. S., Chung, N. Y. F., Li, K. K. W., Poon, W. S., Chan, D. T. M., Shi, Z., Chen, L., Zhou, L., & Ng, H. K. (2014). Loss of CIC and FUBP1 expressions are potential markers of shorter time to recurrence in oligodendroglial tumors. *Modern Pathology*, *27*(3), 332–342. https://doi.org/10.1038/MODPATHOL.2013.165

Ciudad, L., Piulachs, M. D., & Bellés, X. (2006). Systemic RNAi of the cockroach vitellogenin receptor results in a phenotype similar to that of the *Drosophila* yolkless mutant. *The FEBS Journal*, *273*(2), 325–335. https://doi.org/10.1111/J.1742-4658.2005.05066.X

Cooley, L., & Theurkauf, W. E. (1994). Cytoskeletal Functions During *Drosophila* Oogenesis. *Science*, *266*(5185), 590–596. https://doi.org/10.1126/SCIENCE.7939713

Donato Tanaka, E., & Piulachs, M. D. (2012). Dicer-1 is a key enzyme in the regulation of oogenesis in panoistic ovaries. *Biology of the Cell*, *104*(8), 452–461. https://doi.org/10.1111/BOC.201100044

Elshaer, N., & Piulachs, M. D. (2015). Crosstalk of EGFR signalling with Notch and Hippo pathways to regulate cell specification, migration and proliferation in cockroach panoistic ovaries. *Biology of the Cell*, *107*(8), 273–285. https://doi.org/10.1111/BOC.201500003

Fonseca, R. N. da, Lynch, J. A., & Roth, S. (2009). Evolution of axis formation: mRNA localization, regulatory circuits and posterior specification in non-model arthropods. *Current Opinion in Genetics & Development*, *19*(4), 404–411. https://doi.org/10.1016/J.GDE.2009.04.009

Goff, D. J., Nilson, L. A., & Morisato, D. (2001). Establishment of dorsal-ventral polarity of the Drosophila egg requires capicua action in ovarian follicle cells. *Development (Cambridge, England)*, *128*(22), 4553–4562. https://doi.org/10.1242/DEV.128.22.4553

Guindon, S., & Gascuel, O. (2003). A simple, fast, and accurate algorithm to estimate large phylogenies by maximum likelihood. *Systematic Biology*, *52*(5), 696–704. https://doi.org/10.1080/10635150390235520

Herraiz, A., Belles, X., & Piulachs, M. D. (2014). Chorion formation in panoistic ovaries requires windei and trimethylation of histone 3 lysine 9. *Experimental Cell Research*, *320*(1), 46–53. https://doi.org/10.1016/J.YEXCR.2013.07.006

Herranz, H., Hong, X., & Cohen, S. M. (2012). Mutual repression by bantam miRNA and Capicua links the EGFR/MAPK and Hippo pathways in growth control. *Current Biology□: CB*, *22*(8), 651–657. https://doi.org/10.1016/J.CUB.2012.02.050

Irles, P., Bellés, X., & Piulachs, M. D. (2009). Brownie, a Gene Involved in Building Complex Respiratory Devices in Insect Eggshells. *PLOS ONE*, *4*(12), e8353. https://doi.org/10.1371/JOURNAL.PONE.0008353

Irles, P., Elshaer, N., & Piulachs, M. D. (2016). The Notch pathway regulates both the proliferation and differentiation of follicular cells in the panoistic ovary of *Blattella germanica*. *Open Biology*, *6*(1). https://doi.org/10.1098/rsob.150197

Irles, P., & Piulachs, M. D. (2014). Unlike in Drosophila Meroistic Ovaries, Hippo Represses Notch in *Blattella germanica* Panoistic Ovaries, Triggering the Mitosis-Endocycle Switch in the Follicular Cells. *PLOS ONE*, *9*(11), e113850. https://doi.org/10.1371/JOURNAL.PONE.0113850

Jiménez, G., Guichet, A., Ephrussi, A., & Casanova, J. (2000). Relief of gene repression by Torso RTK signaling: role of capicua in *Drosophila* terminal and dorsoventral patterning. *Genes & Development*, *14*(2), 224. https://doi.org/10.1101/gad.14.2.224

Jiménez, G., Shvartsman, S. Y., & Paroush, Z. (2012). The Capicua repressor – a general sensor of RTK signaling in development and disease. *Journal of Cell Science*, *125*(6), 1383. https://doi.org/10.1242/JCS.092965

Kim, E., Kim, D., Lee, J. S., Yoe, J., Park, J., Kim, C. J., Jeong, D., Kim, S., & Lee, Y. (2018). Capicua suppresses hepatocellular carcinoma progression by controlling the ETV4–MMP1 axis. *Hepatology*, *67*(6), 2287–2301. https://doi.org/10.1002/HEP.29738

Kim, E., Park, S., Choi, N., Lee, J., Yoe, J., Kim, S., Jung, H. Y., Kim, K. T., Kang, H., Fryer, J. D., Zoghbi, H. Y., Hwang, D., & Lee, Y. (2015). Deficiency of Capicua disrupts bile acid homeostasis. *Scientific Reports 2015 5:1*, *5*(1), 1–8. https://doi.org/10.1038/srep08272

Lam, Y. C., Bowman, A. B., Jafar-Nejad, P., Lim, J., Richman, R., Fryer, J. D., Hyun, E. D., Duvick, L. A., Orr, H. T., Botas, J., & Zoghbi, H. Y. (2006). ATAXIN-1 interacts with the repressor Capicua in its native complex to cause SCA1 neuropathology. *Cell*, *127*(7), 1335–1347. https://doi.org/10.1016/J.CELL.2006.11.038

Larkin, M. A., Blackshields, G., Brown, N. P., Chenna, R., Mcgettigan, P. A., McWilliam, H., Valentin, F., Wallace, I. M., Wilm, A., Lopez, R., Thompson, J. D., Gibson, T. J., & Higgins, D. G. (2007). Clustal W and Clustal X version 2.0. *Bioinformatics (Oxford, England)*, *23*(21), 2947–2948. https://doi.org/10.1093/BIOINFORMATICS/BTM404

Lee, C. J., Chan, W. I., Cheung, M., Cheng, Y. C., Appleby, V. J., Orme, A. T., & Scotting, P. J. (2002). CIC, a member of a novel subfamily of the HMG-box superfamily, is transiently expressed in developing granule neurons. *Molecular*

Brain Research, *106*(1–2), 151–156. https://doi.org/10.1016/S0169-328X(02)00439-4

Lee, Y. (2020). Regulation and function of capicua in mammals. *Experimental & Molecular Medicine*, *52*(4), 531–537. https://doi.org/10.1038/s12276-020-0411-3

Lee, Y., Fryer, J. D., Kang, H., Crespo-Barreto, J., Bowman, A. B., Gao, Y., Kahle, J. J., Hong, J. S., Kheradmand, F., Orr, H. T., Finegold, M. J., & Zoghbi, H. Y. (2011). ATXN1 protein family and CIC regulate extracellular matrix remodeling and lung alveolarization. *Developmental Cell*, *21*(4), 746–757. https://doi.org/10.1016/J.DEVCEL.2011.08.017

Livak, K. J., & Schmittgen, T. D. (2001). Analysis of relative gene expression data using real-time quantitative PCR and the 2-ΔΔCT method. *Methods*, *25*(4), 402–408. https://doi.org/10.1006/meth.2001.1262

Lynch, J. A., & Roth, S. (2011). The evolution of dorsal–ventral patterning mechanisms in insects. *Genes & Development*, *25*(2), 107. https://doi.org/10.1101/GAD.2010711

Maestro, O., Cruz, J., Pascual, N., Martín, D., & Bellés, X. (2005). Differential expression of two RXR/ultraspiracle isoforms during the life cycle of the hemimetabolous insect *Blattella germanica* (*Dictyoptera, Blattellidae*). *Molecular and Cellular Endocrinology*, *238*, 27–37. https://doi.org/10.1016/j.mce.2005.04.004

Medioni, C., Mowry, K., & Besse, F. (2012). Principles and roles of mRNA localization in animal development. *Development (Cambridge, England)*, *139*(18), 3263–3276. https://doi.org/10.1242/DEV.078626

Misof, B., Liu, S., Meusemann, K., Peters, R. S., Donath, A., Mayer, C., Frandsen, P. B., Ware, J., Flouri, T., Beutel, R. G., Niehuis, O., Petersen, M., Izquierdo-Carrasco, F., Wappler, T., Rust, J., Aberer, A. J., Aspöck, U., Aspöck, H., Bartel, D., … Zhou, X. (2014). Phylogenomics resolves the timing and pattern of insect evolution. *Science (New York, N.Y.)*, *346*(6210), 763–767. https://doi.org/10.1126/SCIENCE.1257570

Pfaffl, M. W., Horgan, G. W., & Dempfle, L. (2002). Relative expression software tool (REST) for group-wise comparison and statistical analysis of relative expression results in real-time PCR. *Nucleic Acids Research*, *30*(9). https://doi.org/10.1093/NAR/30.9.E36

Pridohl, F., Weißkopf, M., Koniszewski, N., Sulzmaier, A., Uebe, S., Ekici, A. B., & Schoppmeier, M. (2017). *Transcriptome sequencing reveals maelstrom as a novel target gene of the terminal system in the red flour beetle Tribolium castaneum*. https://doi.org/10.1242/dev.136853

Riparbelli, M. G., & Callaini, G. (1995). Cytoskeleton of the *Drosophila* egg chamber: new observations on microfilament distribution during oocyte growth. *Cell Motility and the Cytoskeleton*, *31*(4), 298–306. https://doi.org/10.1002/CM.970310406

Rodrıguez-Muñoz, L., Lagares, C., Gonzalez-Crespo, S., Castel, P., Veraksa, A., & Jimenez, G. (2022a). Noncanonical function of Capicua as a growth termination signal in *Drosophila* oogenesis. *Proceedings of the National Academy of Sciences of the United States of America*, *119*(31). https://doi.org/10.1073/PNAS.2123467119/-/DCSUPPLEMENTAL

Roth, S., & Lynch, J. (2012). Axis Formation: Microtubules Push in the Right Direction. *Current Biology*, *22*(13), R537–R539. https://doi.org/10.1016/j.cub.2012.05.038

Roth, S., & Lynch, J. A. (2009). Symmetry breaking during *Drosophila* oogenesis. *Cold Spring Harbor Perspectives in Biology*, *1*(2). https://doi.org/10.1101/CSHPERSPECT.A001891

Shin, D. H., & Hong, J. W. (2014). Capicua is involved in Dorsal-mediated repression of zerknüllt expression in *Drosophila* embryo. *BMB Reports*, *47*(9), 518. https://doi.org/10.5483/BMBREP.2014.47.9.122

Sun, Q.-Y., & Schatten, H. (2006). Regulation of dynamic events by microfilaments during oocyte maturation and fertilization. *Reproduction (Cambridge, England)*, *131*(2), 193–205. https://doi.org/10.1530/REP.1.00847

Tanaka, A. (1973). General accounts on the oocyte growth and the identification of vitellogenin by means of immunospecificity in the cockroach, *Blattella germanica* (l.). *Development, Growth & Differentiation*, *15*(3), 153–168. https://doi.org/10.1111/J.1440-169X.1973.00153.X

Telfer, W. H. (1975). Development and Physiology of the Oöcyte-Nurse Cell Syncytium. *Advances in Insect Physiology*, *11*(C), 223–319. https://doi.org/10.1016/S0065-2806(08)60164-2

Wilson, M. J., Abbott, H., & Dearden, P. K. (2011). The evolution of oocyte patterning in insects: multiple cell-signaling pathways are active during honeybee oogenesis and are likely to play a role in axis patterning. *Evolution & Development*, *13*(2), 127–137. https://doi.org/10.1111/J.1525-142X.2011.00463.X

Wilson, M. J., & Dearden, P. K. (2013). RNA localization in the honeybee (*Apis mellifera*) oocyte reveals insights about the evolution of RNA localization mechanisms. *Developmental Biology*, *375*(2), 193–201. https://doi.org/10.1016/J.YDBIO.2013.01.001

Zhang, Y., & Kunkel, Joseph. G. (1992). Program of F-actin in the follicular epithelium during oogenesis of the german cockroach, *Blattella germanica*. *Tissue and Cell*, *24*(6), 905–917. https://doi.org/10.1016/0040-8166(92)90025-3

Figure Legends

Figure 1. Phylogenetic analysis of the transcription factor Capicua in insects. The analysis is based in the maximum-likelihood principle with the amino acid substitution model was carried out with the Capicua sequences available in public databases. Only bootstrap values higher than 60 are shown in the main basal nodes. *B. germanica* Capicua sequence is depicted in red-bold. Green branches are species belonging to holometabolous insects and red branches are species belonging to hemimetabolous insects. The complete species name and accession numbers of the sequences are indicated in Table S1. Scale bar indicates the number of substitutions per site.

Figure 2. **Expression and localization of *B. germanica* capicua (Cic)**. (A) Relative expression of *cic* mRNA quantified in ovary (Ov), thoracic ganglia (TG), colleterial glands (CG), fat body (FB), brain (Br) and. midgut (MG) from adult female. (B) Relative expression of *cic* in the ovary during sixth instar nymph and in the adult. The expression in ovaries in the last day of fifth nymphal instar was also measured. Data in A and B are expressed as copies per 1000 copies of *actin-5c*. (C) Immunolocalization of Cic in an ovariole from a 6-day-old sixth instar nymph showing the asymmetric distribution of the

actins in the basal follicle. (D-F) Immunolocalization of Cic in basal follicles from 0-day-old (D), 6-day-old (E), and 8-day-old (F and F') sixth instar nymphs, showing the changes of Cic distribution related to the age of the female, from an accumulation in the oocyte membrane (D, E) to be spreaded through the cytoplasm and into the nucleus (F'). (G) Basal ovarian follicle from a 0-day-old adult showing a weakly labelling for Cic. (H-I) Optical section of basal ovarian follicles from 8-day-old sixth instar nymph (H) and 0-day-old adult (I), showing the distribution and the different level of Cic labelling in the ooplasm and in the follicular cells. The arrows indicate the layer of bacteriocytes endosymbionts. Oo: ooplasm. The anterior pole in C and G is towards the right, in D-F is to the top of the image. Cic: green, F-actin: red, DAPI: blue.

Figure 3. **Cic in ovaries of ds*cic* treated females**. (A) Relative expression of *cic* mRNA in ovaries of ds*cic*-treated sixth instar nymphs and newly emerged adult. ds*cic* was applied to nymphs just after the moult to last instar. Data are expressed as copies of *cic* per 1000 copies of *actin-5c*. (B, B') Cic protein in basal follicles of 8-day-old ds*cic*-treated and (C, C') and dsMock sixth instar nymph. The signal intensity of the different fluorophores is show (B' and C') using the option 2.5D of the Zen 2012 blue edition software from Zeiss. Anterior pole of the basal follicle is towards the right. Cic: green, F-actin: red, DAPI: blue.

Figure 4. Ovarian follicles from ds*cic*-treated nymphs at the day of emergence to the last instar. Basal ovarian follicles (BOF) from 8-day-old ds*cic*-treated sixth instar nymphs, showing a different degree of narrowing in the anterior pole (A, B), and the "fishtail-like" phenotype, with a concentration of F-actin in the posterior pole (C, D). (E-G) Ovarioles from 3-day-old ds*cic*-treated adults, showing the elongated shape of the BOF (E), and the engulfment of the anterior pole of the basal oocyte (F, G) by the follicular epithelia. (H) Sub-basal ovarian follicle from 8-day-old sixth instar nymphs showing the network of F-actins connecting the MTOCs placed in both poles of the oocyte. (I, J) BOF from a 8-day-old ds*cic*-treated sixth instar nymph, showing a big MTOC in the anterior pole. (K) BOF from a 3-day-old ds*cic* treated adult showing the network of F-actins, with a big MTOC in the anterior pole of the oocyte, when, usually at

this age the MTOC and the F-actins network are not detected. (L) Ovarioles from a 7-day-old ds*cic*-treated adult. The basal and sub-basal oocytes were lost (oviposited, arrows) before they complete their development. The ovarioles keep the follicular epithelia that were surrounding those oocytes. In these ovarioles, the first oocyte that remains there shows an hourglass shape (M), and is not possible to detect the stalk separating the ovarian follicles. Anterior pole is towards the left. F-actin: red (except in M, which is white), DAPI: blue.

Figure 5. Localization of oocyte nucleus in ds*cic*-treated sixth instar nymphs. (A) Ovariole from 8-day-old dsMock-treated sixth instar nymphs, showing the localization of oocyte nucleus in the ovarian follicles along the ovariole. The image results from the composition of three pictures. (B) Basal ovarian follicle from 8-day-old ds*cic*-treated females showing the posterior position of the oocyte nucleus. (C, D) The loss of the stalks determines the disorganization of the ovarian follicles in the vitellarium that show a mis-localization of the oocyte nuclei (arrowhead). (E- E'') The image shows two fused oocytes resulting in a one ovarian follicle with two nuclei. The arrowhead in the images indicates the place where it should be placed the stalk. The anterior pole is up towards the left. The oocyte nucleus labelled by anti-Eya antibody (green); F-actin: red; DAPI: Blue.

Figure 6. Pathways involved in insect oogenesis affected by *cic* depletion.
(A) mRNA relative expression of different genes (*EGFR, notch, delta, hippo, tailless* and *dorsal*) in ovaries of 8-day-old ds*cic*-treated sixth instar nymphs. Data represent normalized values against dsMock controls (reference value = 1) (n = 3) (*) indicates statistically significant change P(H1) = 0.000. (B) Basal ovarian follicle from 8-day-old dsMock-treated sixth instar nymph, showing the EGFR protein diffused through the ooplasm, showing a high labelling around and inside the oocyte nucleus. (C) Basal ovarian follicle of ds*cic*-treated nymph, the EGFR localization appeared restricted to the central region of the oocyte around the nucleus and towards the oocyte ventral side. F-actin: red; DAPI: Blue, EGFR protein: Green.

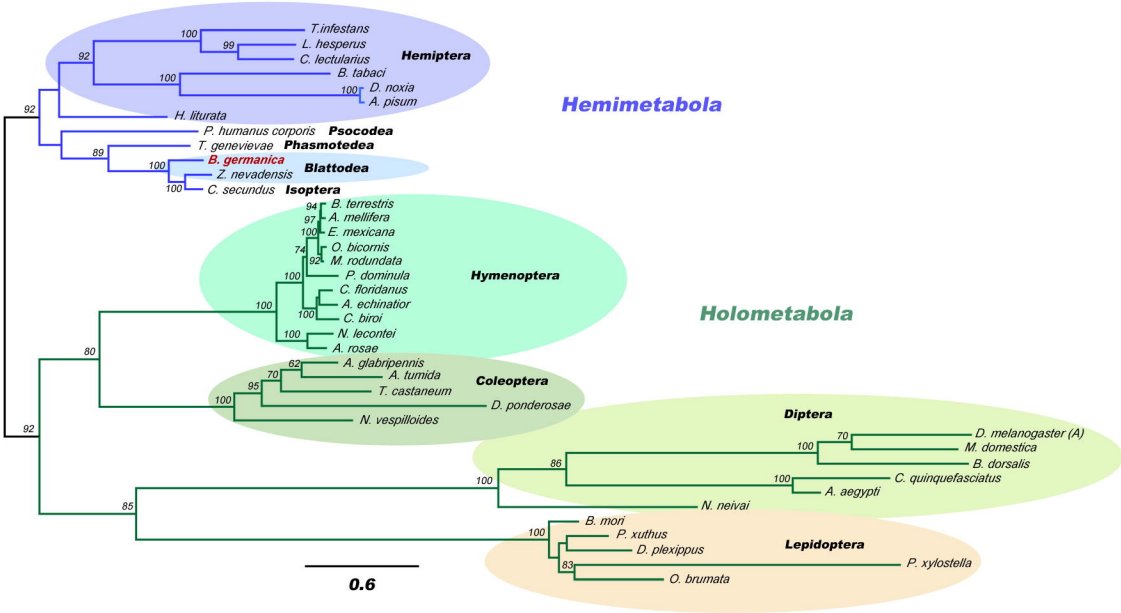
Hemimetabola
Holometabola
Hemiptera
T.infestans
L. hesperus
C. lectularius
B. tabaci
D. noxia
A. pisum
H. liturata
Psocodea
P. humanus corporis
Phasmotedea
T. genevievae
Blattodea
B. germanica
Z. nevadensis
Isoptera
C. secundus
Hymenoptera
B. terrestris
A. mellifera
E. mexicana
O. bicornis
M. rodundata
P. dominula
C. floridanus
A. echinatior
C. biroi
N. lecontei
A. rosae
Coleoptera
A. glabripennis
A. tumida
T. castaneum
D. ponderosae
N. vespilloides
Diptera
D. melanogaster (A)
M. domestica
B. dorsalis
C. quinquefasciatus
A. aegypti
N. neivai
Lepidoptera
B. mori
P. xuthus
D. plexippus
P. xylostella
O. brumata
0.6

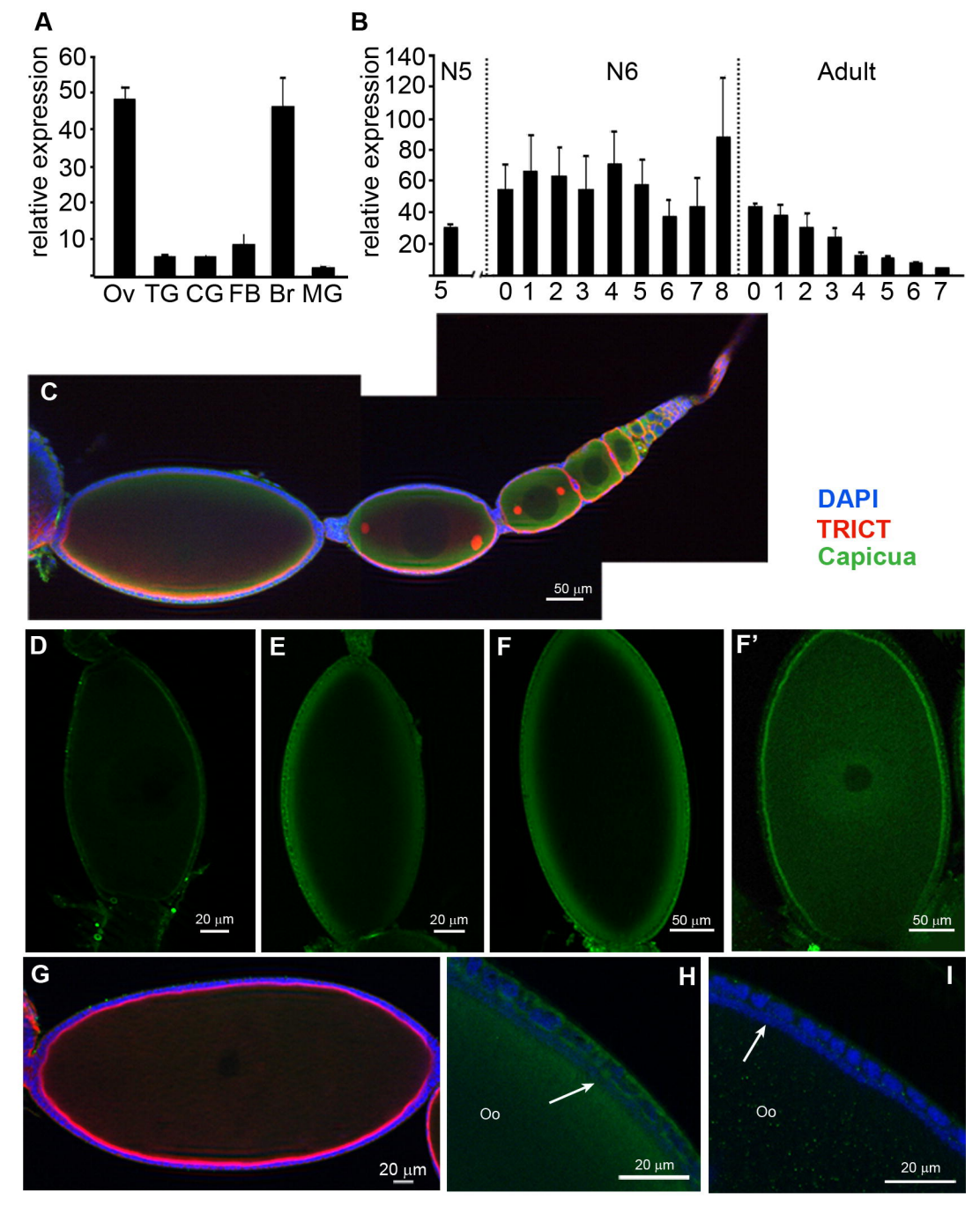
A
relative expression
60
50
40
30
20
10
Ov TG CG FB Br MG
B
relative expression
140
120
100
80
60
40
20
N5
N6
Adult
5
0 1 2 3 4 5 6 7 8 0 1 2 3 4 5 6 7
C
50 µm
DAPI
TRICT
Capicua
D
20 µm
E
20 µm
F
50 µm
F'
50 µm
G
20 µm
H
Oo
20 µm
I
Oo
20 µm

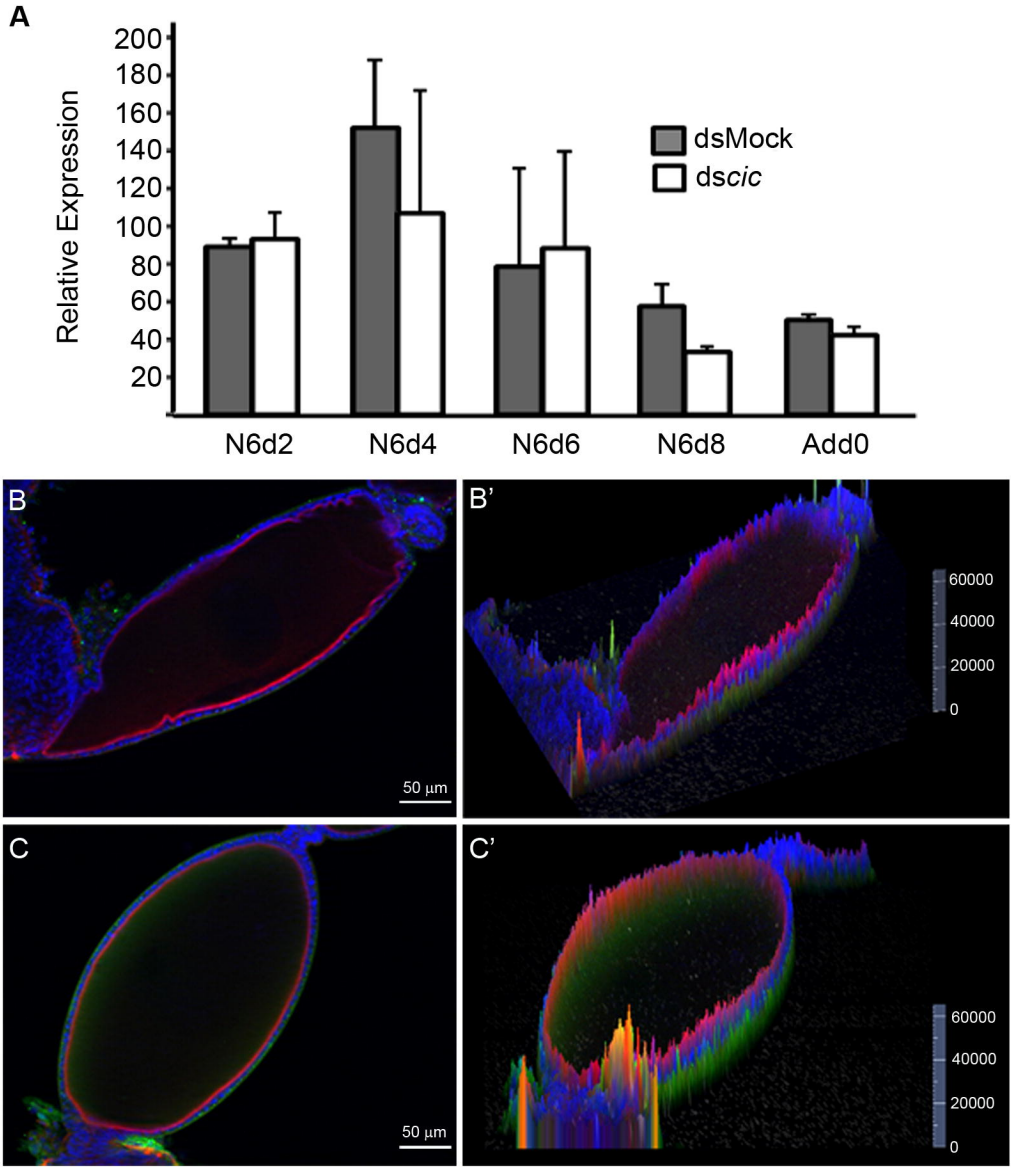
A
Relative Expression
200
180
160
140
120
100
80
60
40
20
dsMock
dscic
N6d2
N6d4
N6d6
N6d8
Add0
B
50 µm
B'
60000
40000
20000
0
C
50 µm
C'
60000
40000
20000
0

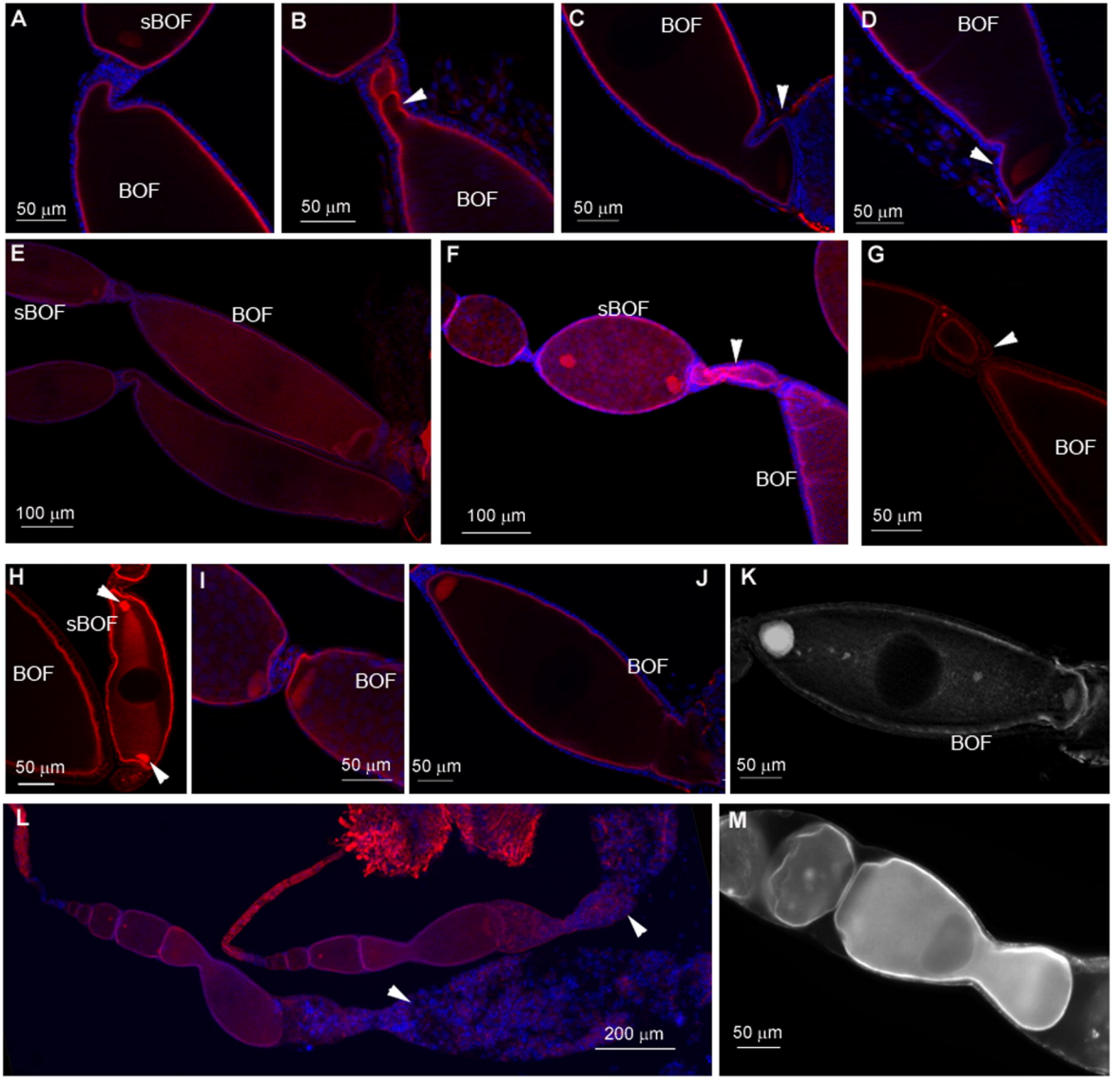
A
sBOF
BOF
50 µm
B
BOF
50 µm
C
BOF
50 µm
D
BOF
50 µm
E
sBOF
BOF
100 µm
F
sBOF
BOF
100 µm
G
BOF
50 µm
H
sBOF
BOF
50 µm
I
BOF
50 µm
J
BOF
50 µm
K
BOF
50 µm
L
200 µm
M
50 µm

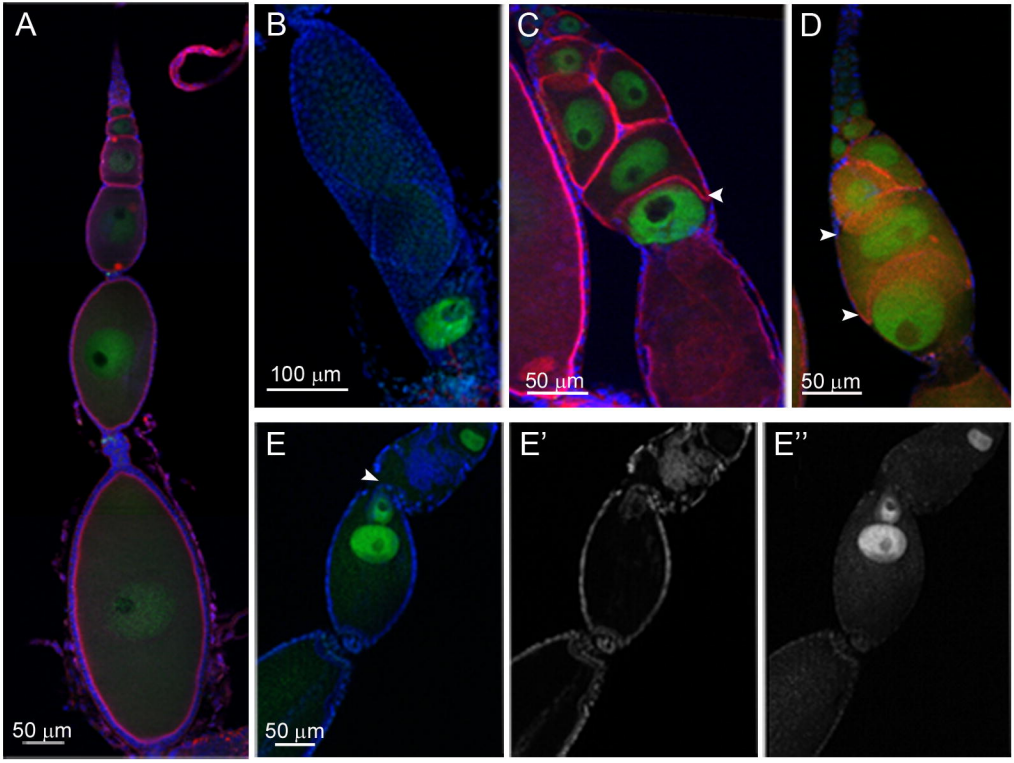
A
B
100 µm
C
50 µm
D
50 µm
50 µm
E
50 µm
E'
E''

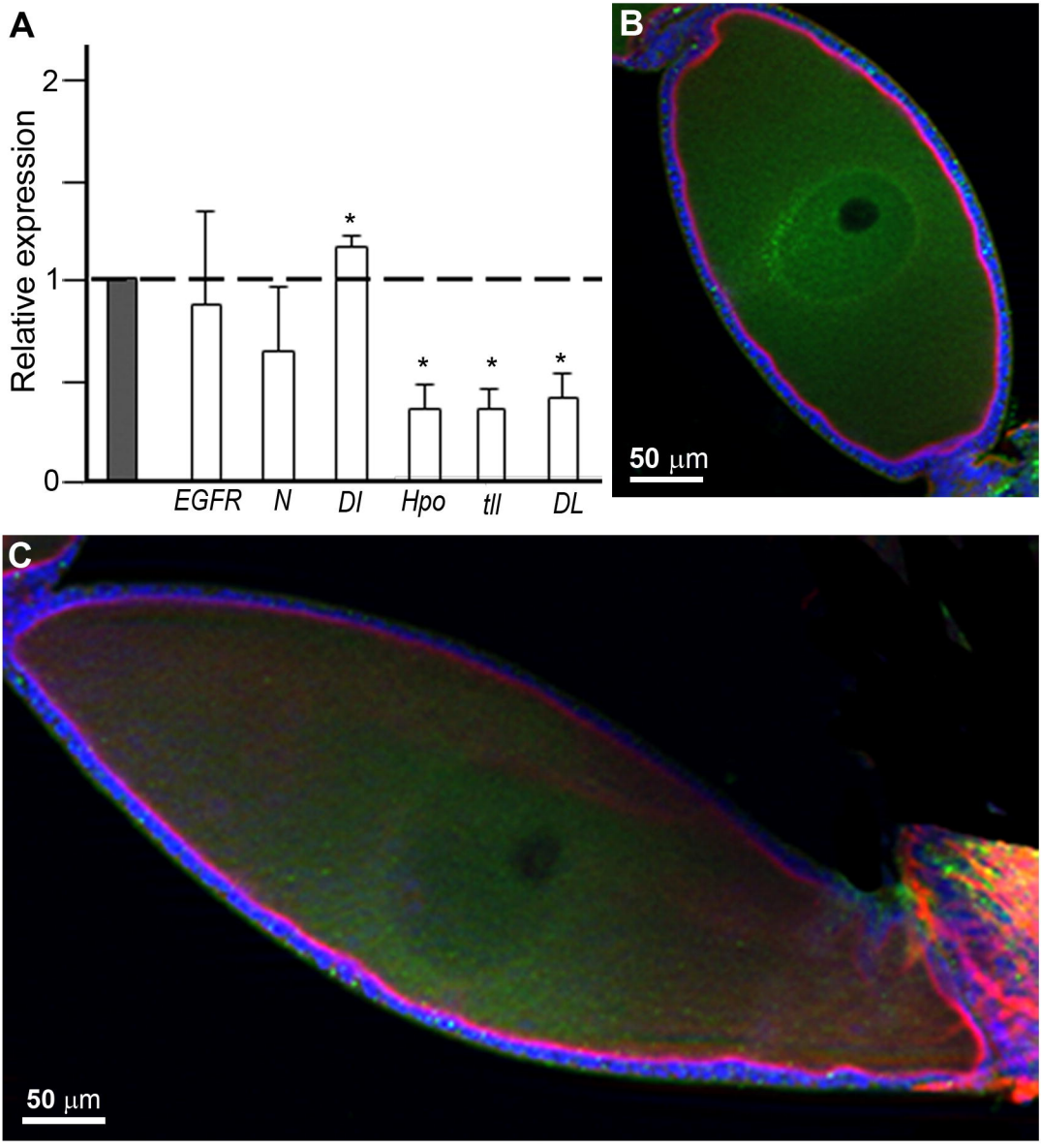
A
Relative expression
2
1
0
*
*
*
*
EGFR
N
Dl
Hpo
tll
DL
B
50 μm
C
50 μm